Proposing a new performance index to identify the effect of spark energy and pulse frequency simultaneously to achieve high machining performance in WEDM

Ibrahem Maher & Ahmed A. D. Sarhan

The International Journal of Advanced Manufacturing Technology

ISSN 0268-3768
Volume 91
Combined 1-4

Int J Adv Manuf Technol (2017)
91:433-443
DOI 10.1007/s00170-016-9680-3

Springer

Int J Adv Manuf Technol (2017) 91:433–443
DOI 10.1007/s00170-016-9680-3

ORIGINAL ARTICLE

Proposing a new performance index to identify the effect of spark energy and pulse frequency simultaneously to achieve high machining performance in WEDM

Ibrahem Maher[1] · **Ahmed A. D. Sarhan**[2,3]

Received: 10 August 2016 / Accepted: 31 October 2016 / Published online: 22 November 2016

Abstract Wire electrical discharge machining (WEDM) is a manufacturing process whereby a desired shape is obtained using electrical discharges (sparks). WEDM demands high cutting rate and high quality to improve machining performance for manufacturing hard materials. The machining performance of computer-controlled WEDM is directly dependent on spark energy and pulse frequency parameters including discharge voltage, peak current, pulse duration, and charging time. In this paper, a new performance index to measure the effects of spark energy and pulse frequency on machining performance is proposed. Moreover, the effects of electric process parameters on performance measures including cutting speed, surface roughness, and white layer thickness are introduced.

Keywords WEDM-CCM · Spark energy · Pulse frequency · Duty factor · Performance index

1 Introduction

Computer numeric controlled (CNC) wire electrical discharge machining (WEDM) is among the more widely known and applied nontraditional machining processes in industry today. In this procedure, improvements to the process mechanism and control have rapidly been taking place. CNC-WEDM can machine harder, electrically conductive (higher strength, corrosive and wear resistant, and difficult-to-machine) materials like tool steel, titanium, metal matrix composites (MMCs), and cemented carbides [1]. Besides machining electrically conductive workpieces, some WEDM work has also been reported on insulating ceramics and non-conductive materials [2, 3]. With WEDM, it is also possible to machine complicated shapes that cannot otherwise be achieved using traditional machining processes, such as turning, milling, and grinding [4, 5].

Productivity and surface quality are the most important performance parameters in CNC-WEDM. In addition, productivity controls the overall cost-effectiveness of the machining process, while quality impacts the functional value of products. Productivity is expressed as cutting speed, while surface quality is expressed through surface roughness and white layer thickness. The importance of these performance parameters is relative and mainly depends on spark energy and pulse frequency parameters [6]. Practically, productivity increases with increasing spark energy (voltage, current, and pulse duration). On the other hand, surface roughness and white layer thickness would increase with increasing discharge voltage, current, and pulse width [7, 8].

Several efforts have been made to find the ideal machining conditions to enhance productivity and achieve high product quality by increasing the cutting rate and decreasing the surface roughness [9, 10]. It has been revealed that cutting speed increases as pulse width increases, and surface roughness decreases as the time between the two pulses decreases. El-Hofy [11] and Levy and Maggi [12] showed that during WEDM, a thin heat-affected zone layer of 1 μm at 5-μJ spark energy to 25 μm at high spark energy is formed. To attain low surface roughness and small white layer thickness, low electrical discharge parameters are required. However, such parameters lower the cutting rate in

✉ Ibrahem Maher
ibrahemmaher@eng.kfs.edu.eg

✉ Ahmed A. D. Sarhan
ah_sarhan@yahoo.com

[1] Department of Mechanical Engineering, Faculty of Engineering, Kafrelsheikh University, Kafrelsheikh 33516, Egypt

[2] Centre of Advanced Manufacturing and Material Processing, Department of Mechanical Engineering, Faculty of Engineering, University of Malaya, Kuala Lumpur 50603, Malaysia

[3] Department of Mechanical Engineering, Faculty of Engineering, Assiut University, Assiut 71516, Egypt

WEDM. This indicates that a high cutting rate with minimum surface defects is difficult to attain from a single-parameter setting. To achieve efficient machining, mathematical modeling between WEDM parameters and performance characteristics should be available to manufacturers. Two kinds of approaches, theoretical and empirical, are commonly used for WEDM modeling [13]. Owing to the simplified and unavoidable assumptions, the theoretical models yield large errors between the predicted and experimental results. On the other hand, empirical models are limited to specific experimental conditions.

Many efforts to improve process performance have been stated in literature regarding electrothermal concepts. Among these efforts, theoretical [14–16], numerical [17, 18], or empirical methods [19, 20] with different performance parameters and guesstimate results are used to improve the machining process. As previously mentioned, WEDM efficiency mostly depends on the generation and distribution of spark energy within the discharge zone [21, 22]. In practice, efficient WEDM control implies variation of spark energy parameters and pulse frequency parameters, which can be controlled by peak current, pulse-on time, and pulse-off time. However, it is very difficult to study the effect of spark energy and pulse frequency individually on machining performance. This suggests that a high cutting rate with minimum surface defects is difficult to attain from a single-parameter setting. For this reason, in this research work, we proposed a new, simple performance index to study the effect of spark energy in conjunction with pulse frequency at different duty factors on machining characteristics to achieve high machining performance in CNC-WEDM. This can be achieved by weighing the spark energy using the duty factor.

2 Analysis of EDM pulse generator

2.1 Cycle energy

CNC wire electrical discharge machining (CNC-WEDM), sometimes informally also referred to as spark machining, spark eroding, burning, wire burning, or wire erosion, is a manufacturing process whereby a desired shape is obtained using electrical discharges (sparks), while the NC table can make X-Y movements (Fig. 1a, b). Material is removed from the workpiece by a series of rapidly repeating current discharges between the wire electrode and the workpiece, separated by a dielectric liquid, and is subject to electric voltage (Fig. 2a, b) [23].

Figure 3 illustrates the WEDM machine components and a detailed description of the pulse generator used in WEDM. In a pulse generator, the capacitor is charged from a DC source (V_o). As long as the voltage in the capacitor does not reach the breakdown voltage of the dielectric medium under machining conditions (T_{off}), the capacitor (C) continues to charge. Once breakdown voltage (V_d) is reached, the capacitor starts discharging and a spark is established between the tool and workpiece, leading to machining. Such discharge continues as long as the spark can be sustained. Once the voltage becomes too low (V_d^*) to sustain the spark, capacitor charging would continue, as shown in Fig. 4 [11].

During an electrical discharge, the voltage and current impulses vary with time. Electric impulses are determined with the following values: discharge voltage (V_d), pulse duration (T_{on}), pulse-off time (T_{off}), pulse cycle time (T_c), discharge current (IP), pulse frequency (F), and duty factor (DF). The most important WEDM parameters are spark energy and duty factor. The spark energy determines the chip size, and it is the value of electrical energy per one spark, which can be expressed by Eq. (1).

$$E_s = V_d \times \mathrm{IP} \times T_{on} \tag{1}$$

According to Eq. (1), spark energy is influenced by the discharge voltage, discharge current, and pulse duration. The discharge voltage depends on the paired wire electrode and workpiece materials [24]. The discharge current and pulse duration control the spark intensity (Fig. 5a, b). The spark energy determines the spark size and, hence, the chip size. High spark intensity leads to long sparks, thus increasing the cutting speed and chip size but decreasing the surface finish as shown in Fig. 5a [25].

The other most important parameter associated with electrical parameters and that significantly influences WEDM performance is pulse frequency (F) or duty factor (DF). The duty factor determines the weight and number of pulses (Eqs. 2 and 3). The duty factor is a percentage of the ratio of pulse duration to total cycle time. In machines with duty factor settings, the pulse interval is set indirectly by setting the pulse duration and duty factor. Pulse frequency is used to set the pulse interval on some machines and to determine the number of chips per second.

$$F = 1/(T_{on} + T_{off}) \tag{2}$$

$$\mathrm{DF} = T_{on}/(T_{on} + T_{off}) = T_{on} \times F \tag{3}$$

Selecting a spark microsecond cycle time depends on workpiece thickness, flushing condition, and required surface quality. High pulse frequency leads to short sparks and, hence, decreased chip size (Fig. 5b). This condition is consequently recommended to improve surface finish. Low pulse frequency leads to long sparks and, hence, increased chip size (Fig. 5a), so it is recommended for increasing cutting speed [26].

2.2 Cutting speed

The molten crater can be assumed to have hemispherical shape with a radius r that forms due to a single spark

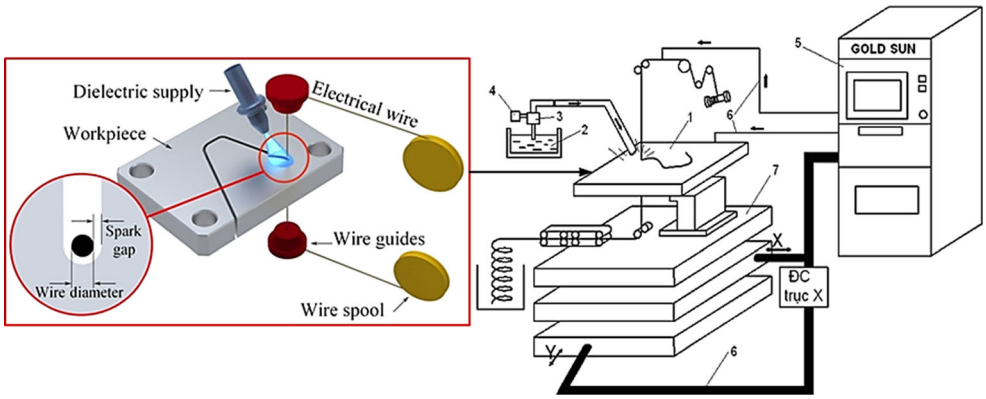

Fig. 1 WEDM-CCM machine components (*1* workpiece, *2* dielectric fluid, *3* pump, *4* pressure gaga, *5* power supply, *6* X-Y control unit, *7* machine table)

(Fig. 5a). Hence, volume removal (VR) in a single spark can be expressed as follows [11]:

$$\mathrm{VR} = 2\pi r^3/3 \tag{4}$$

Material removal in a single spark is proportional to spark energy. Thus,

$$\mathrm{VR}\ \alpha\ E_s \tag{5}$$

The material removal rate is the ratio of material removed in a single spark to cycle time. Thus,

$$\mathrm{MRR} = \mathrm{VR}/T_c \tag{6}$$

$$T_c = T_{on} + T_{off} \tag{7}$$

$$\mathrm{MRR}\ \alpha\ E_s/(T_{on} + T_{off})$$

$$\mathrm{MRR} = \mathrm{CS} \times w \times b \tag{8}$$

where CS is the cutting speed, w is the kerf width, and b is the workpiece depth.

$$\mathrm{CS} = \mathrm{MRR}/w \times b$$

$$\mathrm{CS}\ \alpha\ E_s/(T_{on} + T_{off}) \tag{9}$$

From Eqs. (3) and (9), we get the following:

$$\mathrm{CS}\ \alpha\ E_s \times F \tag{10}$$

2.3 Surface roughness

Surface roughness is the most well-known product quality issue in WEDM. In WEDM, no two sparks can take place side-by-side. They occur completely randomly so that over time, uniform average material removal occurs over the entire wire electrode contact length. For the sake of simplicity, it is assumed that sparks occur side-by-side as shown in Fig. 5. Thus,

$$\mathrm{Ra}\ \alpha\ r \tag{11}$$

From Eqs. (4) and (5)

$$r = (3\mathrm{VR}/2\pi)^{1/3} = (3KE_s/2\pi)^{1/3} \tag{12}$$

$$\mathrm{Ra}\ \alpha\ (E_s)^{1/3} \tag{13}$$

It is noted from Eq. (13) that surface roughness increases with increasing spark energy [11]. Moreover,

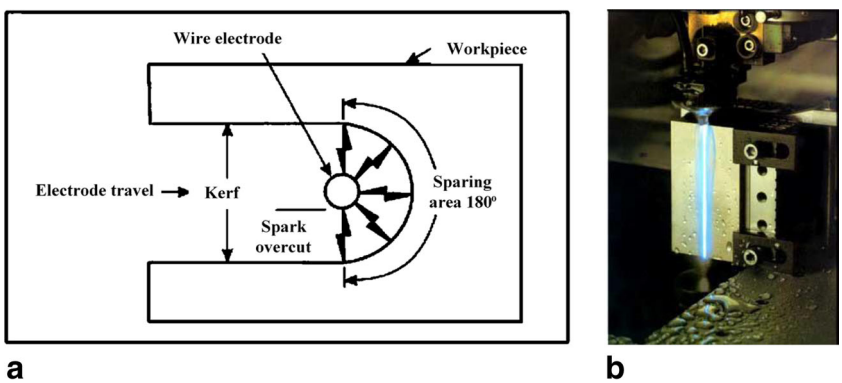

Fig. 2 WEDM discharge sparks

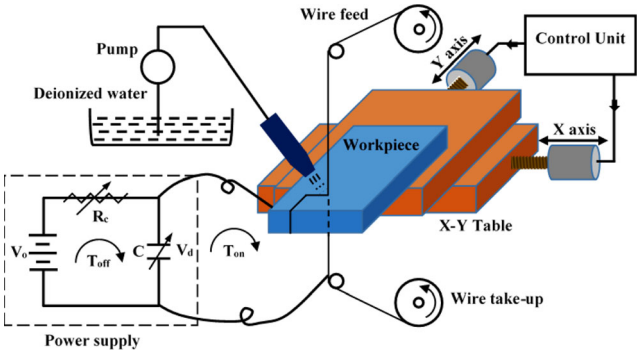

Fig. 3 Detailed description of the pulse generator and machine components

pulse frequency has considerable effect on surface roughness (see Fig. 5).

2.4 White layer thickness

During WEDM, the discharge temperature can reach up to 12,000 °C, and metallurgical changes happen in some of the workpiece surface layers [11]. As such, the zone under the machined surface can be annealed. Moreover, some molten material does not get into the dielectric fluid and chills quickly, mainly by heat conduction throughout most of the workpiece, resulting in a hard surface. The annealed layer depth is generally proportional to the spark energy used in the cutting process. It is around 50 μm for finish cutting to approximately 200 μm for high cutting rates (Fig. 6) [27]. A recast layer appears in different spark erosion conditions and contains many pockmarks, globules, cracks, and microcracks. Researchers have carried out several investigations and noted that this layer is obvious under all machining conditions [28, 29].

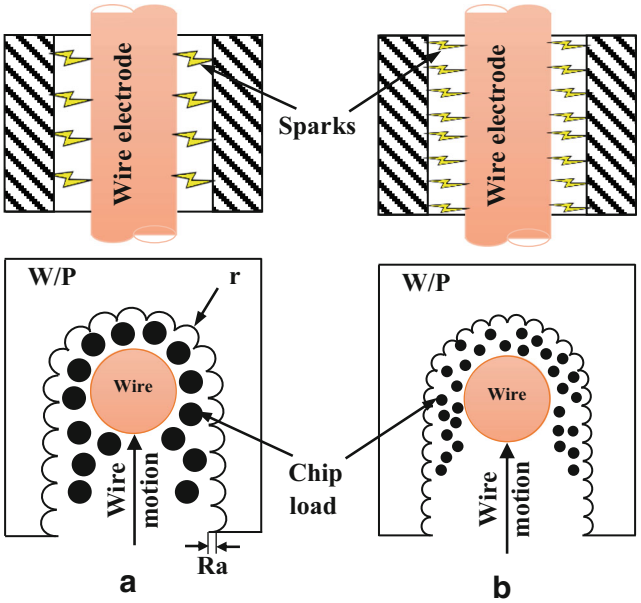

Fig. 5 Chip size and load at different spark energies and pulse frequencies. **a** High spark energy with low pulse frequency. **b** Low spark energy with high pulse frequency

3 Experimental details

3.1 Experimental setup

The experiments were performed using a computer numerical control (CNC) Sodick AQ325L WEDM machine tool (Fig. 7). The wire electrode employed is a wire (Brass wire (60/40) coated with 5 μm of CuZn alloy (30/70)), with 0.2-mm diameter, tensile strength of 875 N/mm^2, elongation of 0.2, and electric conductivity of 20% IACS for machining titanium alloy grade 5 (Ti6Al4V) under the machining conditions listed in Table 1.

The machining parameters, including peak current (IP), pulse width (T_{on}), and charging time (T_{off}), were selected for this study based on Eqs. (1) and (2) to investigate the effect of

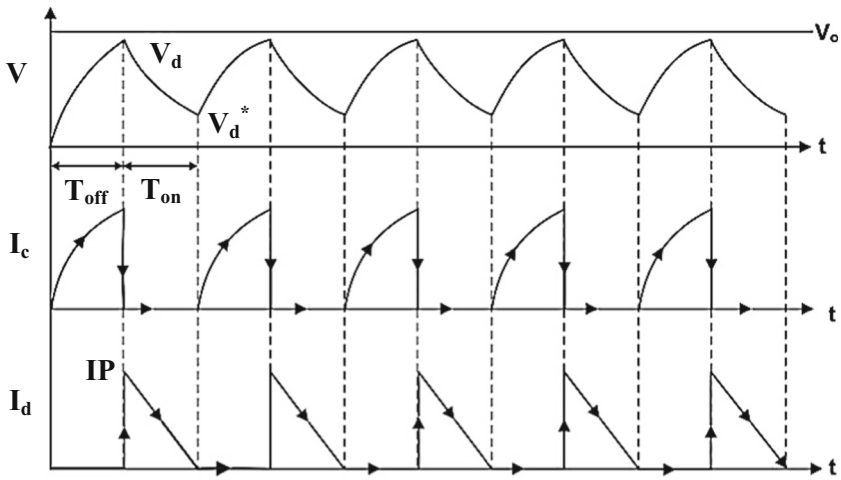

Fig. 4 Analysis of EDM pulse generator

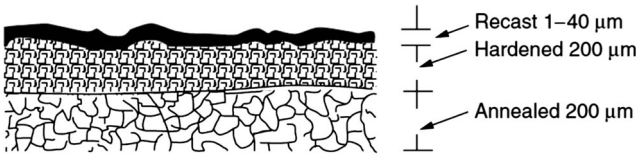

Fig. 6 EDM machined surface heat-affected zone

spark energy and pulse frequency parameters on machining performance, i.e., cutting speed (CS), surface roughness (Ra), and white layer thickness (WLT). The machining parameter levels (Table 1) were selected based on previous experiments with the working range and levels of the WEDM process parameters by using the one-factor-at-a-time approach. The other machining parameters were kept constant (main voltage $V_o = 100$ V, gap voltage $V_d = 20$ V, wire tension WT = 6 N, and wire speed WS = 3 m/min) as recommended by the machine maker.

3.2 Specimen preparation

The workpiece material used is titanium alloy grade 5 (Ti6Al4V) with 100 × 100 × 20-mm dimensions, which was machined into 5 × 5 × 20 mm for each specimen. The chemical composition of titanium alloy was achieved by EDX machine as shown in Table 2. The electrical resistivity and thermal conductivity of titanium alloy were 17.8 × 10^{-5} Ω cm and 6.7 W/(m K), respectively.

Table 1 Levels of machining parameters

Machining parameter	Symbol	Units	Levels		
			1	2	3
Peak current	IP	A	16	17	-
Pulse-on time	T_{on}	μs	0.2	0.3	0.4
Pulse-off time	T_{off}	μs	0.5	0.9	1.3

The samples were ground with 400, 800, 1200, 2000, and 4000 grit silicon carbide paper and subsequently polished with 3 and 1 μm diamond suspension liquid, followed by mirror polishing with 0.05 Alumina suspension. The samples were then cleaned in an ultrasonic agitator in acetone at 30 °C for 15 min, carefully rinsed and cleaned in distilled water, and dried to remove contamination so as to acquire a uniform surface [30].

3.3 Measurements

Cutting speed was recorded directly from the WEDM machine tool monitor. The average cutting speed was calculated from the three data points recorded under the same conditions. The surface roughness was measured with a stylus-based profilometer (Mitutoyo SJ-201, 99.6% accuracy). The average surface roughness was calculated for three different measurements under

Fig. 7 WEDM machine

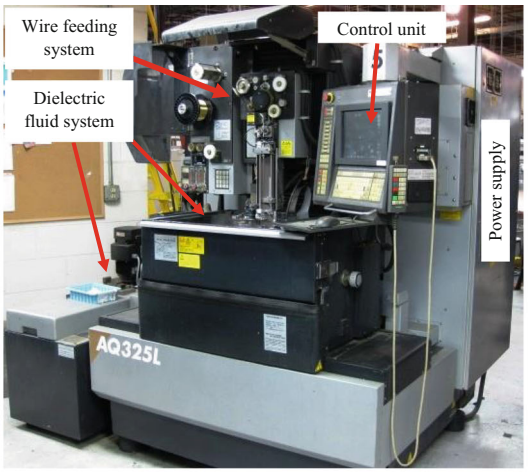

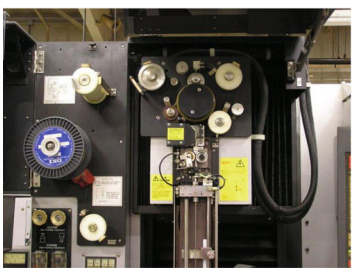

Table 2 Chemical compositions of titanium alloy (grade 5)

Element	Al	V	Fe	O	C	Ti
Weight, wt (%)	5.65	3.93	0.13	0.11	0.08	90.1

the same conditions with a roughness width cutoff of L_c = 0.8 mm based on standard ISO 4287:1997. The average white layer thickness was calculated from three measurements using an image processing program (ImageJ).

3.4 Surface characterization

Microscopic surface examinations after each grinding and finishing step were carried out using Olympus BX 61 light optical microscopy (OM). A scanning electron microscope (SEM) equipped with energy-dispersive X-ray spectroscopy (EDS) (Hitachi tabletop microscope TM3030) was used to examine the surface microstructural and topographical characteristics and white layer thickness of the machined part.

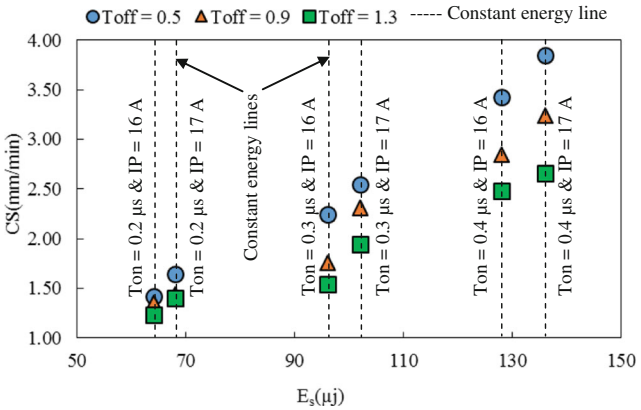

Fig. 8 Influence of spark energy parameters on cutting speed

4 Results, analysis, and discussion

A total of 18 sets of data were selected to study the effect of spark energy parameters and pulse frequency on machining performance, as demonstrated in Table 3.

4.1 Cutting speed analysis

Figure 8 represents the effect of the spark energy parameters (IP, T_{on}, and T_{off}) on cutting speed. As Fig. 8 indicates, an increase of peak current and pulse duration leads to higher cutting speed. The same conclusion can be drawn from the

Table 3 Measured CS (mm/min), Ra (μm), and WLT (μm) at different machining conditions

Machining parameters			Performance factors			Performance outcomes											
IP (A)	T_{on} (μs)	T_{off} (μs)	E_s (μJ)	DF (%)	E_sDF index	CS (mm/min)				Ra (μm)				WLT (μm)			
						1	2	3	avg	1	2	3	avg	1	2	3	avg
16	0.2	0.5	64	28.6	1829	1.4	1.35	1.5	1.42	2.2	2.2	2.29	2.23	6.16	4.75	6.07	5.66
		0.9	64	18.2	1164	1.37	1.3	1.4	1.36	2.2	2.11	2.15	2.15	6.28	5.23	3.38	4.96
		1.3	64	13.3	853	1.33	1.18	1.2	1.24	2.19	2.11	1.98	2.09	5.27	3.52	4.25	4.35
	0.3	0.5	96	37.5	3600	2.21	2.15	2.38	2.25	2.63	2.74	2.69	2.69	9.93	11.78	8.56	10.09
		0.9	96	25.0	2400	1.82	1.92	1.53	1.76	2.55	2.41	2.51	2.49	7.02	8	7.56	7.53
		1.3	96	18.8	1800	1.37	1.57	1.69	1.54	2.38	2.31	2.28	2.32	6.02	5.58	6.77	6.12
	0.4	0.5	128	44.4	5689	3.41	3.28	3.6	3.43	2.98	3.21	2.99	3.06	16.6	16.19	16.25	16.35
		0.9	128	30.8	3938	2.73	2.92	2.9	2.85	2.89	2.84	2.85	2.86	12.25	12.32	13.37	12.65
		1.3	128	23.5	3012	2.33	2.59	2.52	2.48	2.76	2.59	2.71	2.69	11.1	10.65	11.44	11.06
17	0.2	0.5	68	28.6	1943	1.67	1.57	1.69	1.64	2.33	2.28	2.32	2.31	7.73	6.08	5.98	6.60
		0.9	68	18.2	1236	1.46	1.37	1.5	1.44	2.29	2.18	2.2	2.22	6.43	5.32	5.37	5.71
		1.3	68	13.3	907	1.36	1.45	1.4	1.40	2.32	2.09	2.09	2.17	5.56	5.07	4.96	5.20
	0.3	0.5	102	37.5	3825	2.6	2.54	2.5	2.55	2.86	2.82	2.78	2.82	11.09	12.68	10.68	11.48
		0.9	102	25.0	2550	2.22	2.39	2.31	2.31	2.7	2.63	2.66	2.66	10.33	11.72	9.78	10.61
		1.3	102	18.8	1913	1.97	1.9	1.98	1.95	2.4	2.45	2.52	2.46	8.73	9.32	7.85	8.63
	0.4	0.5	136	44.4	6044	3.73	3.92	3.9	3.85	3.34	3.14	3.27	3.25	20.57	19.38	19.86	19.94
		0.9	136	30.8	4185	3.29	3.1	3.33	3.24	2.99	2.89	2.89	2.92	14	17.58	15.47	15.68
		1.3	136	23.5	3200	2.71	2.59	2.68	2.66	2.69	2.78	2.75	2.74	13.48	13.01	11.65	12.71

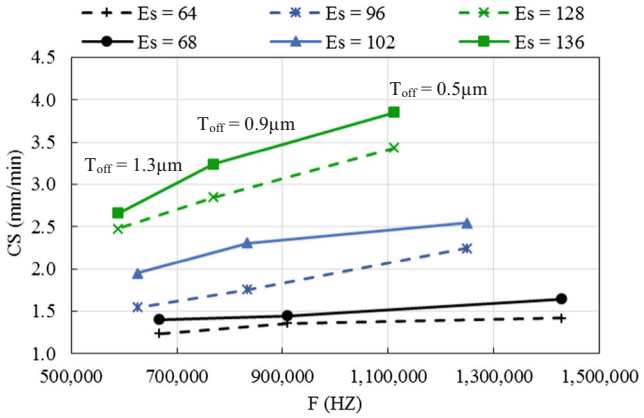

Fig. 9 Influence of cycle frequency on cutting speed

cutting speed equation (10) presented in Sect. 2.2. Moreover, Fig. 8 shows that pulse duration has a great effect on cutting speed followed by peak current. In addition, pulse-off time has a considerable effect on speed as shown in Fig. 9. The spark discharge energy obtained from Eq. (1) increases with the increase of discharge current and pulse duration. But, at the same spark energy level (constant energy line represented by a dashed line in Fig. 8), the cutting speed decreases with increasing pulse-off time. Increasing pulse-off time leads to decreasing pulse frequency at the same energy levels; hence, the cutting speed decreases as shown in Fig. 9.

From Eqs. (1) and (2) and Figs. 8 and 9, both the pulse frequency and spark energy affect the cutting speed. However, it is very difficult to study the effect of each one individually on cutting speed. Therefore, a new performance index is proposed in this study to merge the effect of pulse frequency with spark energy. This can be done by normalizing the spark energy parameters by multiplying the spark energy with the duty factor (E_s × DF).

Figure 10 displays the change in cutting speed at different performance index levels. According to Fig. 10, cutting speed increases linearly with the increase in the new performance index. When the discharge energy parameters (V_d, IP, and/or

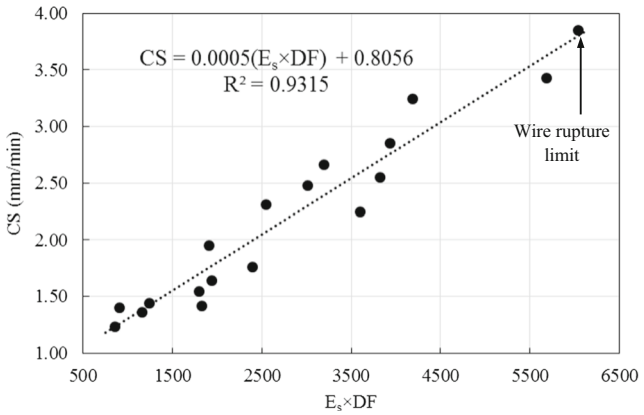

Fig. 10 Experimental influence of weighted spark energy on the cutting speed

Table 4 ANOVA table for cutting speed

Source	DF	Sum of squares	Mean square	*F*-ratio	*p* value
Es × DF	1	9.8929	9.8929	217.63	0.000
Residual error	16	0.7273	0.0455		
Total	17	10.6202			

T_{on}) and/or the duty factor change, the new performance index changes accordingly. Figure 10 also shows the wire rupture limit based on the new performance index.

A regression technique was employed to understand the effect of the performance index on cutting speed, surface roughness, and white layer thickness. From the regression models, one can obtain the relationship between the criterion variable and the predictive variable. The linear regression, correlation coefficient, and coefficient of determination are all related. Based on some assumptions, each one provides different types of information. The coefficient of determination represents the correlation coefficient's squares. The correlation coefficient indicates whether or not the two variables move in the same or opposite directions and the degree of linear association. So, the regression technique along with the coefficient of determination was used to obtain the relationship of the criterion variable (cutting speed, surface roughness, and white layer thickness) and the predictive variable (performance index).

Table 4 represents the statistical analysis and effects of performance index on cutting speed. According to ANOVA, at 95% confidence level ($p < 0.05$) when p is less than 0.05, the performance index significantly affects cutting speed.

The empirical equation is presented as follows:

$$\mathrm{CS} = 0.8056 + 0.0005(E_s \times \mathrm{DF}) \tag{14}$$

Equation (14) indicates that cutting speed increases with increasing performance index. The analytical relationship between cutting speed and the new performance index has a high coefficient of determination

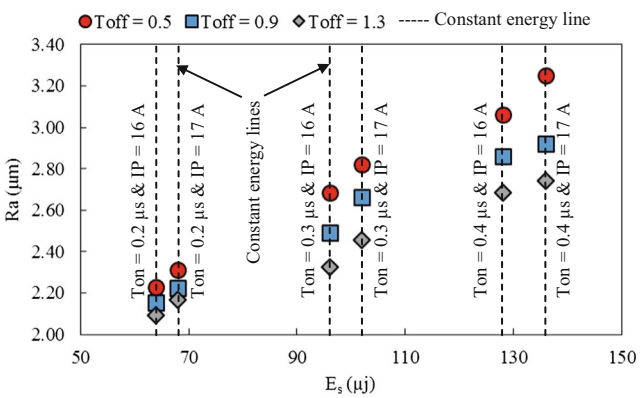

Fig. 11 Influence of spark energy parameters on surface roughness

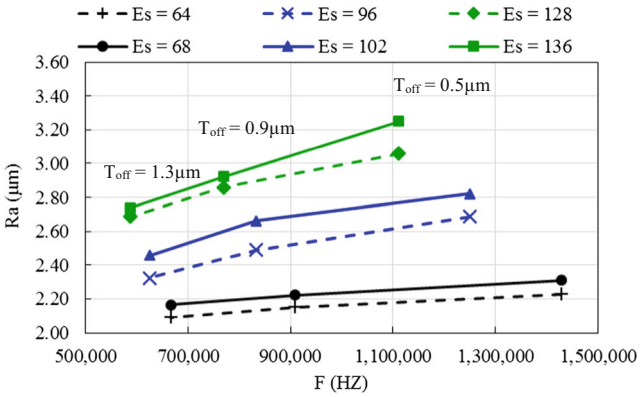

Fig. 12 Influence of cycle frequency on surface roughness

(R^2 = 0.93). The coefficient of determination is a measure of how well an analytical model is likely to predict future outcomes. This correlation coefficient is calculated by dividing the covariance of two variables by their standard deviations. The predicted R^2 value (93.2%) and adjusted R^2 value (92.7%) match the experimental results. The adjusted R^2 determines the amount of deviation about the mean that is described by the model [31].

Therefore, the new performance index is accurate and can be used as an index for monitoring, predicting, and controlling the cutting speed performance measure as well as identifying the wire rupture limit.

4.2 Surface quality analysis

This section presents the analysis of the effects of the spark energy and pulse frequency parameters on surface quality. Figure 11 shows the influence of the spark energy parameters on surface roughness. From this figure, the pulse duration, peak current, and pulse-off time affect the surface roughness. Also, this figure indicates that an increase of discharge power (IP) and/or discharge duration (T_{on}) results in increased

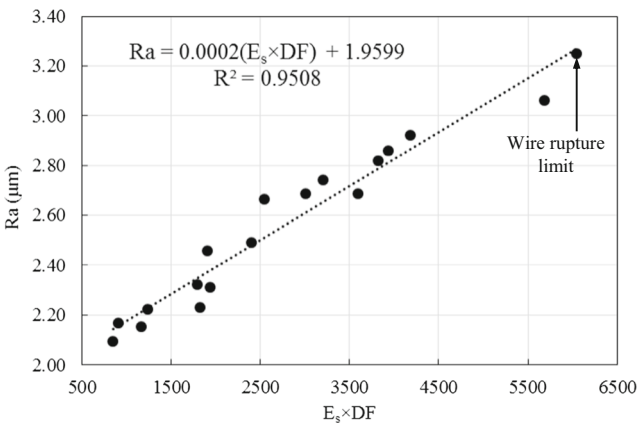

Fig. 13 Experimental influence of weighted spark energy on the surface roughness

Table 5 ANOVA table for surface roughness

Source	DF	Sum of squares	Mean square	*F*-ratio	*p* value
Es × DF	1	1.8872	1.8872	309.03	0.000
Residual error	16	0.0977	0.0061		
Total	17	1.9849			

surface roughness. As the discharge energy increases, the thermal energy concentration on the workpiece increases, which results in large craters; hence, the surface roughness increases. The same conclusion can be drawn from the analytical relationship between surface roughness and discharge energy. Figure 12 displays the influence of cycle frequency on surface roughness at different spark energy levels. It is clear from Fig. 12 that pulse frequency has a small effect on surface

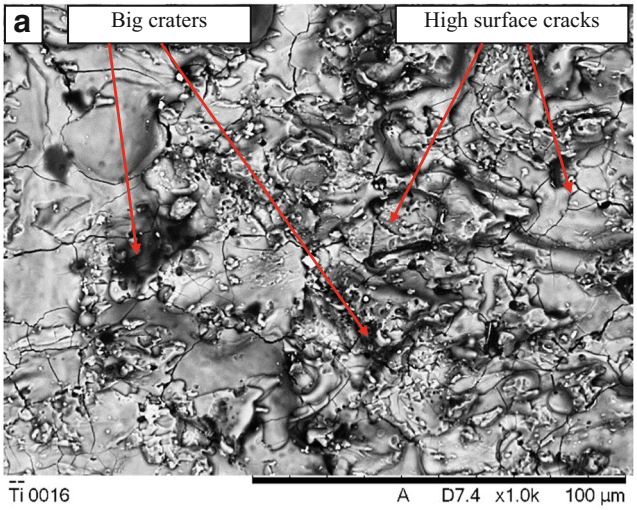

(a) At high levels of spark energy and duty percent

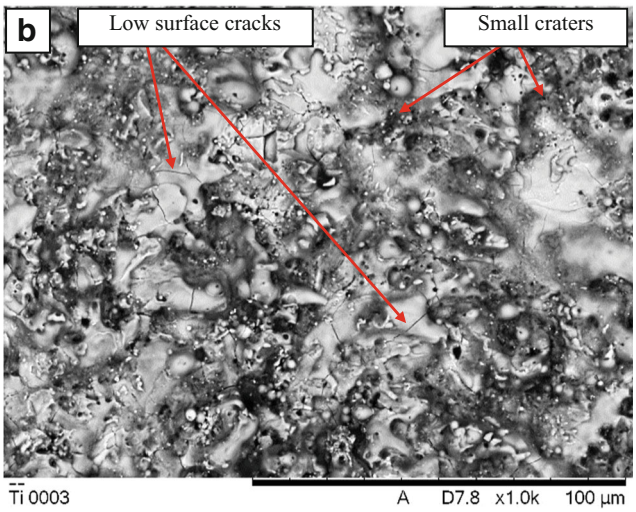

(b) At low level of spark energy and duty percent

Fig. 14 SEM micrograph at the extreme levels of spark energy and duty factor. **a** At high levels of spark energy and duty percent. **b** At low level of spark energy and duty percent

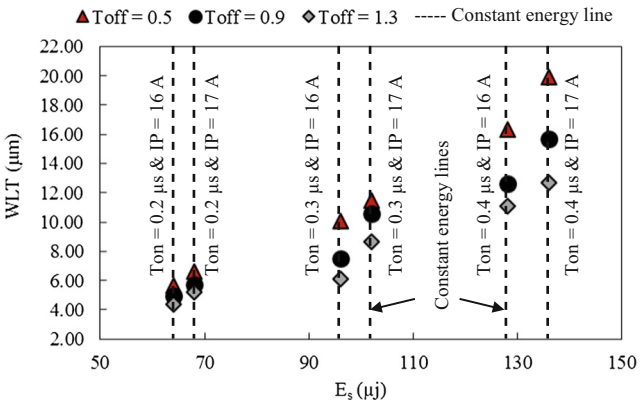

Fig. 15 Influence of spark energy parameters on white layer thickness

roughness. Surface roughness increases with increasing pulse frequency at the same spark energy level. Also, according to Figs. 11 and 12, it is hard to analyze the effect of spark energy and pulse frequency together on surface roughness. Thus, the proposed performance index can be used to study the effect of both spark energy and pulse frequency simultaneously.

Figure 13 shows the relation between surface roughness and the proposed performance index. Surface roughness increases linearly with increasing the proposed performance index. When the electrical process parameters (IP, T_{on}, and T_{off}) change, the proposed performance index changes accordingly. Moreover, the analytical relationship between surface roughness and the proposed performance index has a high coefficient of determination ($R^2 = 0.951$), high adjusted coefficient of determination ($R^2 = 0.958$), and low p value ($p < 0.05$) as per Table 5 (ANOVA); hence, the performance index has a significant effect on surface roughness. By using regression on the recorded data, the prediction model for surface roughness is expressed as follows:

$$\mathrm{Ra} = 1.9599 + 0.0002(E_s \times \mathrm{DF}) \tag{15}$$

In Eq. (15), surface roughness increases with increasing performance index.

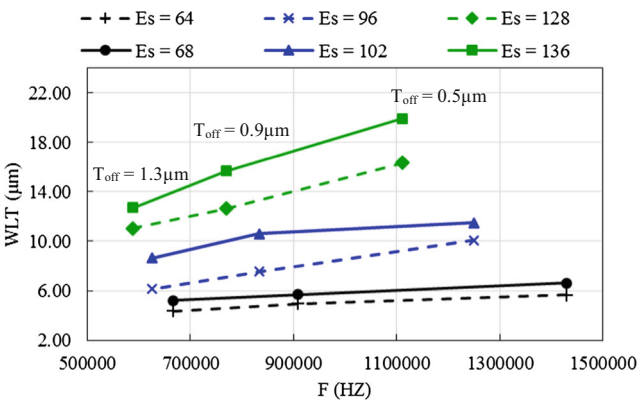

Fig. 16 Influence of cycle frequency on white layer thickness

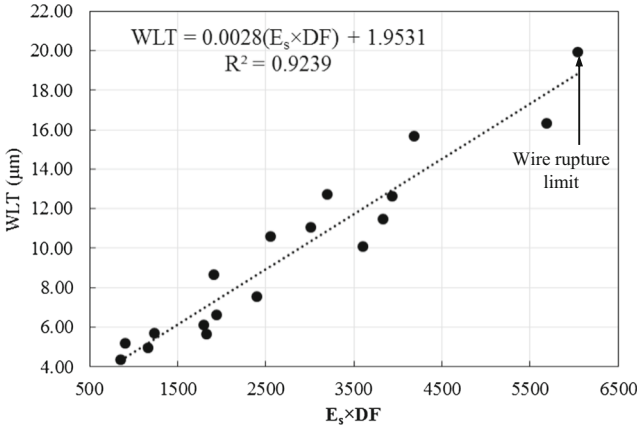

Fig. 17 Experimental influence of weighted spark energy on the white layer thickness

Figure 14a, b shows the SEM of two surfaces at two different levels of the proposed performance index. These two surfaces represent two extreme cases of process conditions under the highest performance index (Fig. 14a) and the lowest performance index (Fig. 14b). Bigger craters and more surface cracks due to larger amounts of molten work material at each spark erosion can be identified on WEDM surfaces (Fig. 14a). On the other hand, crater size and number of cracks reduce drastically on surfaces machined with a low performance index, as shown in Fig. 14b. Thus, the proposed performance index is accurate and can be used for monitoring, predicting, and controlling surface roughness performance measures.

4.3 White layer thickness analysis

This section introduces the analysis of the effects of spark energy and pulse frequency parameters on white layer thickness. The pulse duration has more prominent influence on white layer thickness than discharge current, but pulse-off time has minor influence on white layer thickness (Fig. 15). However, white layer thickness increases as pulse-off time decreases at the same energy level (the constant energy line is represented by a dashed line in Fig. 15). Figure 16 indicates the influence of cycle frequency on white layer thickness at different spark energy levels. White layer thickness increases with increasing pulse frequency, as per Fig. 16. This is because the increase in pulse frequency increases the heat generated on the workpiece surface; hence, the white layer thickness increases. Moreover, according to Figs. 15 and 16, it is difficult to study the dependence of white

Table 6 ANOVA table for white layer thickness

Source	DF	Sum of squares	Mean square	F-ratio	p value
Es × DF	1	314.53	314.53	194.21	0.000
Residual error	16	25.91	1.62		
Total	17	340.45			

layer thickness on spark energy and pulse frequency simultaneously. On the other hand, the proposed performance index can be used to study the effect of both spark energy and pulse frequency on the white layer thickness concurrently.

Figure 17 shows the relation between white layer thickness and the proposed performance index. The white layer thickness increases linearly with increasing the proposed performance index. When the spark energy and frequency parameters (IP, T_{on}, and T_{off}) change, the proposed performance index changes accordingly, leading to a change in white layer thickness. Moreover, the effect of performance index on white layer thickness is introduced statistically in the ANOVA table (Table 6). According to ANOVA, at 95% confidence level ($p < 0.05$), the performance index has significant effect on white layer thickness. The empirical equation based on the regression technique is presented as follows:

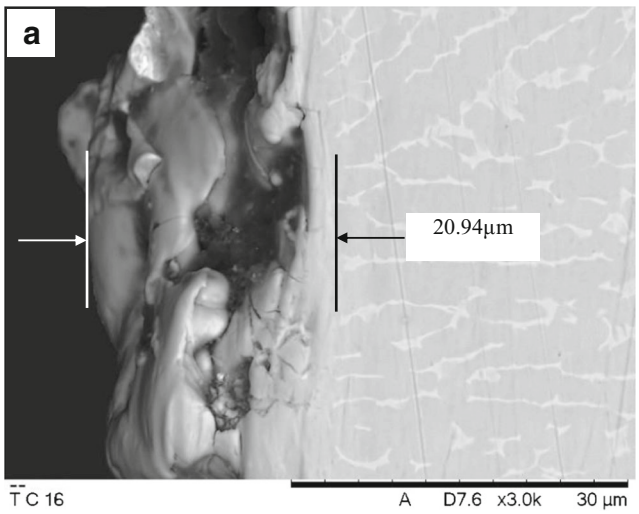

(a) At high levels of spark energy and pulse frequency

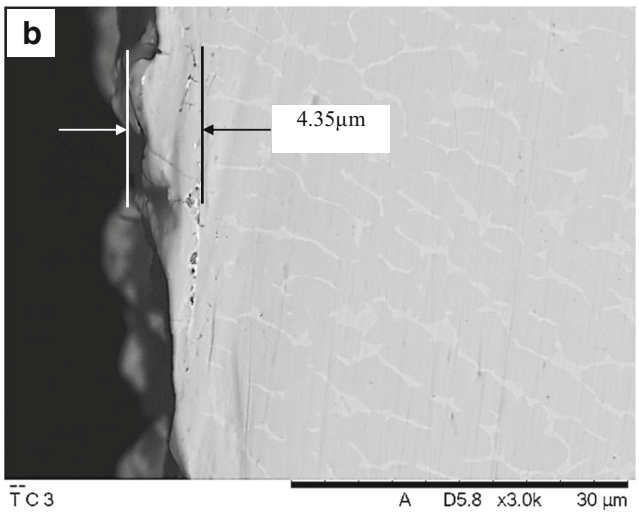

(d) At low levels of spark energy and pulse frequency

Fig. 18 SEM micrograph of the edge at different levels of spark energy and pulse frequency. **a** At high levels of spark energy and pulse frequency. **b** At low levels of spark energy and pulse frequency

$$\mathrm{WLT} = 1.9531 + 0.0028(E_s \times \mathrm{DF}) \tag{16}$$

Equation (16) indicates that white layer thickness increases with increasing performance index. The analytical relationship between white layer thickness and proposed performance index has a high coefficient of determination ($R^2 = 0.924$) and high adjusted coefficient of determination (R^2 (adj.) = 91.9%).

Metallographic investigations show that there is a recast layer (white layer) at low and high discharge energies (Fig. 18). Figure 18 shows the SEM of the edge for two samples at extreme performance index. Figure 18a shows the white layer thickness at high performance index, while Fig. 18b shows the white layer thickness at low performance index. In principle, increasing discharge energy increases the performance index, hence increasing recast layer thickness (Fig. 18). Therefore, the proposed performance index is accurate and can be used for monitoring, predicting, and controlling the white layer thickness performance measure as well as avoiding wire rupture.

5 Conclusion

Based on the previously mentioned analytical and experimental investigations, the machining performance of CNC-WEDM is directly dependent on spark energy parameters (IP, V_d, and T_{on}) and duty factor parameters (T_{on} and T_{off}). The theoretical analysis and experimental results present good agreement and high potential to be used in future research to control and predict CNC-WEDM machining conditions. The proposed performance index ($E_s \times$ DF) much more conveniently correlates the performance parameters (CS, Ra, and WLT) with the spark energy and duty factor parameters in the CNC-WEDM process. By applying the proposed performance index ($E_s \times$ DF), it appears that using a lower spark setting with higher pulse cycle settings will reduce chip size and produce better flushing. This could lead to faster cutting with good surface finish and less wire rupture. Moreover, the new performance index gives a good indication of the wire rupture limit.

Acknowledgements This research was funded by the University of Malaya research grant no: RP039B-15AET and the University of Malaya Postgraduate Research Grant (PPP) No: PG020-2013B.

References

1. Davim JP (2008) Machining fundamentals and recent advances. Springer, London
2. Muttamara A, Fukuzawa Y, Mohri N, Tani T (2003) Probability of precision micro-machining of insulating Si3N4 ceramics by EDM. J Mater Process Technol 140:243–247

3. Wüthrich R, Fascio V (2005) Machining of non-conducting materials using electrochemical discharge phenomenon—an overview. Int J Mach Tools Manuf 45:1095–1108
4. Maher I, Sarhan AAD, Hamdi M (2015) Review of improvements in wire electrode properties for longer working time and utilization in wire EDM machining. Int J Adv Manuf Technol 76:329–351
5. Cheng X, Yang XH, Huang YM, Zheng GM, Li L (2014) Helical surface creation by wire electrical discharge machining for micro tools. Robot Comput Integr Manuf 30:287–294
6. Maher I, Ling LH, Sarhan AAD, Hamdi M (2015) Improve wire EDM performance at different machining parameters—ANFIS modeling, 8th Vienna International Conference on Mathematical Modelling (MATHMOOD 2015), IFAC, Vienna University of technology, Vienna, Austria, pp. 105–110
7. Yeh C-C, Wu K-L, Lee J-W, Yan B-H (2013) Study on surface characteristics using phosphorous dielectric on wire electrical discharge machining of polycrystalline silicon. Int J Adv Manuf Technol 69:71–80
8. Maher I, Sarhan AAD, Marashi H (2016) Effect of electrical discharge energy on white layer thickness of WEDM process, Reference Module in Materials Science and Materials Engineering, Elsevier
9. Yan M-T, Liu Y-T (2009) Design, analysis and experimental study of a high-frequency power supply for finish cut of wire-EDM. Int J Mach Tools Manuf 49:793–796
10. Gökler Mİ, Ozanözgü AM (2000) Experimental investigation of effects of cutting parameters on surface roughness in the WEDM process. Int J Mach Tools Manuf 40:1831–1848
11. El-Hofy H (2005) Advanced machining processes. McGraw-Hill, New York
12. Levy GN, Maggi F (1990) WED machinability comparison of different steel grades. CIRP Ann Manuf Technol 39:183–185
13. Patil N, Brahmankar PK (2010) Determination of material removal rate in wire electro-discharge machining of metal matrix composites using dimensional analysis. Int J Adv Manuf Technol 51:599–610
14. Liao YS, Yu YP (2004) Study of specific discharge energy in WEDM and its application. Int J Mach Tools Manuf 44:1373–1380
15. Singh A, Ghosh A (1999) A thermo-electric model of material removal during electric discharge machining. Int J Mach Tools Manuf 39:669–682
16. Cabanes I, Portillo E, Marcos M, Sánchez JA (2008) On-line prevention of wire breakage in wire electro-discharge machining. Robot Comput Integr Manuf 24:287–298
17. Salah NB, Ghanem F, Atig KB (2006) Numerical study of thermal aspects of electric discharge machining process. Int J Mach Tools Manuf 46:908–911
18. Izquierdo B, Sánchez JA, Plaza S, Pombo I, Ortega N (2009) A numerical model of the EDM process considering the effect of multiple discharges. Int J Mach Tools Manuf 49:220–229
19. Dekeyser W, Snoeys R, Jennes M (1988) Expert system for wire cutting EDM, based on pulse classification and thermal modeling. Robot Comput Integr Manuf 4:219–224
20. Lee C-S, Heo E-Y, Kim J-M, Choi I-H, Kim D-W Electrode wear estimation model for EDM drilling, Robotics and Computer-Integrated Manufacturing
21. Gostimirovic M, Kovac P, Sekulic M, Skoric B (2012) Influence of discharge energy on machining characteristics in EDM. J Mech Sci Technol 26:173–179
22. Salonitis K, Stournaras A, Stavropoulos P, Chryssolouris G (2009) Thermal modeling of the material removal rate and surface roughness for die-sinking EDM. Int J Adv Manuf Technol 40:316–323
23. Jahan M (2013) Micro-electrical discharge machining. In: Davim JP (ed) Nontraditional machining processes. Springer, London
24. Ferreira J (2007) A study of die helical thread cavity surface finish made by Cu-W electrodes with planetary EDM. Int J Adv Manuf Technol 34:1120–1132
25. Portt J (1992) Introduction to wire EDM. John Portt, Michigan
26. Jameson EC (2001) Electrical discharge machining. Society of Manufacturing Engineers, Dearborn, Michigan
27. McGeough, J A (1988) Electrodischarge machining. In: Advanced methods of machining. Shapman and Hall, London, New York
28. Ramasawmy H, Blunt L, Rajurkar KP (2005) Investigation of the relationship between the white layer thickness and 3D surface texture parameters in the die sinking EDM process. Precis Eng 29: 479–490
29. Jangra K, Grover S, Aggarwal A (2011) Simultaneous optimization of material removal rate and surface roughness for WEDM of WC-Co composite using grey relational analysis along with Taguchi method. Int J Ind Eng Comput 2:479–490
30. Zipperian DC (2011) Metallographic handbook. PACE Technologies, Arizona
31. Montgomery DC, Runger GC (2003) Applied statistics and probability for engineers, 3 ed., Wiley.